Lifting Surface Theory of Axial Compressor Blade Rows: Part I—Subsonic Compressor

OLUFEMI OKUROUNMU*
University of Lagos, Lagos, Nigeria
AND
JAMES E. MCCUNE†
MIT, Cambridge, Mass.

The authors' three-dimensional, inviscid linearized lifting line theory of compressible flow past a lifting axial compressor rotor is developed into a lifting surface theory. A solution is constructed by distributing bound vortices of varying strength in the radial and chordwise directions over the surfaces of the rotor blades, and expressions are obtained for the induced velocities everywhere. The general solution shows features of axisymmetric through-flow actuator disk theory, in addition to describing the details of the flow dependent on the detailed blade loading and geometry. Attention is focused on the case where the relative Mach number is everywhere subsonic, and for this case, the quasi-two-dimensional approximation to the flow at each radial section is extracted from the general solution. The latter approximation is shown to consist of both the local flow due to an equivalent actuator disk and the local two-dimensional cascade flow at the section. Three-dimensional corrections to these approximations are then obtained, and are identified as being primarily due to the vortices concentrated in the blade wakes. Camber-line profiles corresponding to prescribed loading distributions are computed, and the influence of the wakes on these profiles demonstrated.

Nomenclature

(r, x, θ) = right-handed coordinate system denoting radial, axial, and azimuthal directions, respectively
ω = angular velocity of rotor
U = axial velocity of airstream far upstream of rotor
U_r = local velocity relative to the blade
(ρ, z, θ) = $(\omega r/U, \omega x/U, \theta)$ = dimensionless coordinates
ζ = helical coordinate, defined by $\zeta = \theta - z$
B = number of blades
ζ_t = sawtooth periodic function of θ and z, such that $\partial\zeta_t/\partial\theta = 1$, and $\partial\zeta_t/\partial z = -1$ everywhere, and with discontinuities of magnitude $2\pi/B$ at $\zeta = \pm\pi/B$, $\pm 3\pi/B \ldots$
M = axial Mach number of undisturbed flow
β = $(1-M^2)^{1/2}$
(r_H, r_T) = hub and tip radius, respectively
η = $r/r_T = \rho/\rho_T$
h = r_H/r_T, ratio of hub to tip radius
$\Phi_1(\rho, z, \theta)$ = lifting line velocity potential
$\Phi(\rho, z, \theta)$ = lifting surface velocity potential
$\Gamma(r)$ = total integrated blade loading at each radius
$\bar{\Gamma}$ = mean loading across the blade span, defined by

$$\bar{\Gamma} = \frac{2}{1-h^2}\int_h^1 \eta\Gamma(\eta)\,d\eta$$

$G_{nB}(nB\rho)$ = wake function corresponding to lifting line theory
K_{nk} = radial eigenvalues
$R_{nB}(K_{nk}\eta)$ = orthonormal radial eigenfunctions
Γ_{nk} = coefficients of the Fourier-Bessel expansion of $\Gamma(r)$ in a series of the orthonormal characteristic functions, $R_{nB}(K_{nk}\eta)$
H_{nk} = coefficients of the Fourier-Bessel expansion of $G_{nB}(nB\rho)$ in a series of the orthonormal characteristic functions, $R_{nB}(K_{nk}\eta)$
$\phi(\rho)$ = $\tan^{-1}\rho$, complement of local stagger angle
$\gamma(\rho, \xi)$ = strength of distributed vortex system over the chordwise extent of the blades, such that

$$\int_0^{C_{ax}(r)} \gamma(\rho, \xi)\,d\xi/\cos\phi = \Gamma(\rho)$$

$c_{ax}(r)$ = axial projection of the blade chord
$c(r)$ = local blade chord
λ_{nk} = eigenvalue for axial eigenfunctions
$\bar{\gamma}(\xi)$ = local mean blade loading across the span defined by

$$\bar{\gamma}(\xi) = \frac{2}{1-h^2}\int_h^1 [\gamma(\eta, \xi)/\cos\phi]\eta\,d\eta$$

$\chi_{nB}(nB\rho, \xi)$ = $\chi_n(\eta, \xi)$ = wake function corresponding to a bound vortex filament at position $x = \xi$ along the blade chord
$\gamma_{nk}(\xi)$ = coefficients of the Fourier-Bessel expansion of $\gamma(\eta, \xi)/\cos\phi$ in a series of the functions $R_{nB}(K_{nk}\eta)$
$h_{nk}(\xi)$ = coefficients of the Fourier-Bessel expansion of $\chi_n(\eta, \xi)$ in a series of the functions $R_{nB}(K_{nk}\eta)$
(u, v, w) = induced perturbation velocities in the (x, θ, r) directions
y_r = azimuthal distance, measured from the zeroth blade leading edge = $r(\theta - \pi/B)$
(ξ', x') = coordinates measured along the local chordwise direction, from the blade leading edge
y_r' = coordinate orthogonal to x' and r
(u', v') = perturbation velocity components in the (x', y_r') directions
$(\Omega_r, \Omega_\theta, \Omega_z)$ = vorticity components of the flow
ψ = abbreviation for $\theta - \omega\xi/U + M^2/\beta^2(z - \omega\xi/U)$
λ_r^n = two-dimensional limiting form of the axial eigenvalue at radius r
M_r = local relative Mach number at radius r
β_r = $(1-M_r^2)^{1/2}$
μ_r = $(M_r^2-1)^{1/2}$
l_r = local blade spacing, $= 2\pi r/B$
Y = $y_r - \xi\tan\phi + M^2/\beta^2(x-\xi)\tan\phi =$ $y_r + (M_x^2/\beta^2)\tan\phi - (\xi/\beta^2)\tan\phi$
C_{p0} = circumferentially averaged pressure rise coefficient from far upstream to far downstream of the rotor
$g(\xi)$ = blade chordwise loading function, defined by Eq. (41)
I_1, I_2, I_3 = operators defined by Eq. (38)
S_{nk}, S_D = functions defined by Eq. (46)
$\Gamma_m(\eta)$ = modified loading when actual loading has nonzero derivatives at root and tip
D = $(\Gamma_T - \Gamma_H)/\bar{\Gamma}$
$\sigma_{-\infty}$ = reference mass density, far upstream of rotor

Received September 18, 1973; revision received May 17, 1974. The present work was carried out while O. Okurounmu was a Research Engineer at the United Aircraft Research Laboratories, East Hartford, Conn.; with J. E. McCune as a Consultant to the company. Also, a portion of McCune's work was supported by NASA Lewis Research Center, under Grant NGL 22-009-383.

Index categories: Aircraft Aerodynamics (Including Component Aerodynamics); Aircraft Noise, Aerodynamics (Including Sonic Boom); Aircraft Noise, Powerplant.

* Lecturer in Mechanical Engineering.
† Professor of Aeronautics and Astronautics. Member AIAA.

μ_{nk} $= -i\lambda_{nk}$, when λ_{nk} is imaginary

Superscripts

u, d = upstream ($x < 0$); downstream ($x > c_{ax}$), respectively
i = between the blade leading and trailing edges, ($0 \leqq x \leqq c_{ax}$)

Subscripts

ad = refers to induced velocities in the plane of an equivalent actuator disk
$2D$ = local quasi-two-dimensional approximation
$3D$ = three-dimensional corrections to the cascade-through flow theory
(H, T) = hub and tip conditions
$(-\infty, +\infty)$= far upstream and far downstream conditions

I. Introduction

PRESENT practice in the design of compressor blade rows is based largely on the assumption of the applicability of the two-dimensional cascade flow at each blade section, supplemented by additional information obtained from axially symmetric through-flow theories. The latter theories however are only partially successful in giving an adequate picture of the three-dimensional flowfield. For example, they are insensitive to the number of blades of the rotor, since the assumption of axial symmetry implies infinitely many blades.[1] Thus, they fail to account for the effects of the individual trailing vortices behind the blade row.

In the following, a linearized three-dimensional lifting surface theory of axial compressor blade rows is presented. When averaged azimuthally, the theory displays the same features as the axially symmetric through-flow (actuator disk) theory. The general theory reduces, in its two-dimensional limiting form, to the local two-dimensional cascade flow at each blade section, plus an equivalent actuator disk-type flow. This enables us to derive what we have called "three-dimensional corrections" to the above quasi-two-dimensional flow, these being due to the finiteness of the blade spacing and the induced velocity field of the concentrated vortices in the blade wakes. The magnitudes of these latter two effects are studied numerically for a rotor with prescribed chordwise and radial loading distributions.

In the present paper, attention is confined to rotors in which the relative Mach number is everywhere subsonic. In Part 2, transonic rotors will be separately treated. When the loading is uniform radially, there is of course no wake, and the only difference between the cascade-through flow theories and the present theory is in the finiteness of the blade spacing. This effect is shown to be very small. However, when the integrated chordwise loading varies from root to tip, the presence of trailing helical vortex sheets introduces additional induced velocities, which can be quite significant. The induced velocities obtained from the general theory are used to compute the camber-line profiles consistent with the prescribed chordwise load distributions, and the importance of including wake effects is demonstrated.

In an earlier paper,[2] a three-dimensional lifting line theory of axial compressor blade rows was presented. In that theory, each blade was represented by a bound vortex line of varying strength $\Gamma(r)$ along the span. The theory was helpful in providing information for which a detailed knowledge of the loading distribution on the blade was not essential. Thus, it yielded the first-order static pressure rise across the rotor, the fluid turning angles and the first-order torque. By extending the calculations to second order, the losses due to the wakes and acoustic radiation (for supersonic relative Mach numbers) were estimated, and further, these second-order calculations were shown to be consistent with satisfaction of radial equilibrium downstream of the rotor. A shortcoming of the theory was that it could not show how the development of the flowfield depended on the detailed loading on the blades, or provide such information as the pressure distribution on the blades, or the blade camber consistent with prescribed loading profiles. The present theory removes these limitations.

The starting point for the lifting surface theory is the lifting line velocity potential given in Ref. 2 as

$$\Phi_1{}^u(\rho,\theta,z) = \frac{B}{2\pi\beta^2}\left\{\sum_{k=1}^{\infty}\frac{-\Gamma_{ok}}{2\lambda_{ok}}e^{\lambda_{ok}z}R_0(K_{ok}\eta)+\sum_{n=1}^{\infty}\sum_{k=1}^{\infty}\left[(-1)^n\frac{H_{nk}}{\lambda_{nk}}+\frac{i\beta^2(-1)^n}{nB}(\Gamma_{nk}+H_{nk})\right]\times e^{inB\theta}\,e^{(inBM^2/\beta^2+\lambda_{nk})z}R_{nB}(K_{nk}\eta)\right\} \quad (1)$$

$$\Phi_1{}^d(\rho,\theta,z) = \frac{B}{2\pi\beta^2}\left\{\bar{\Gamma}z+\beta^2\Gamma(\eta)\zeta_l+\sum_{k=1}^{\infty}\frac{-\Gamma_{ok}}{2\lambda_{ok}}\times e^{-\lambda_{ok}z}R_0(K_{ok}\eta)+\beta^2\sum_{n=1}^{\infty}\sum_{k=1}^{\infty}(-1)^{2n}\frac{2i}{nB}H_{nk}\,e^{inB\zeta}R_{nB}(K_{nk}\eta)+\sum_{n=1}^{\infty}\sum_{k=1}^{\infty}\left[\frac{(-1)^n}{\lambda_{nk}}H_{nk}-\frac{i\beta^2(-1)^n}{nB}(\Gamma_{nk}+H_{nk})\right]\times e^{inB\theta}\,e^{(inBM^2/\beta^2-\lambda_{nk})z}R_{nB}(K_{nk}\eta)\right\} \quad (2)$$

where the real parts are implied. Equations (1) and (2) represent the velocity potential due to B rotating "spokes" of bound vorticity, plus that associated with their wakes of shed vorticity when $\Gamma \neq$ const.

In these equations, $\rho = \omega r/U$, $z = \omega x/U$, ω is the angular velocity of the rotor and U is the axial velocity of the airstream far upstream of the rotor. (r, x, θ) is a right-handed coordinate system denoting the radial, axial, and azimuthal directions, respectively. The superscripts u, d denote upstream ($z < 0$) and downstream ($z > 0$), respectively. The coordinate ζ is a helical coordinate defined by $\zeta = \theta - z$, after Goldstein[3] and Reissner.[4] Also, $\eta = r/r_T$ where r_T is the radius of the blade tip. The symbol h_{nk} in Ref. 2 has been replaced here by H_{nk}. Correspondingly, the wake functions, which in the above reference were denoted by $\chi_{nB}(nB\rho)$ are here denoted by $G_{nB}(nB\rho)$. This slight change in notation is made so as to distinguish these quantities from their corresponding lifting surface analogs, for which we shall retain the symbols h_{nk} and χ_{nB} which now however depend on the axial coordinate, as we shall see subsequently. All other symbols in Eqs. (1) and (2) have exactly the same meaning as in Ref. 2. For ease of reference in what follows, we repeat the following:

1) The H_{nk}'s are the coefficients of the Fourier-Bessel expansion of the wake functions $G_{nB}(nB\rho)$ in a series of the orthonormal characteristic functions $R_{nB}(K_{nk}\eta)$, while the Γ_{nk}'s are the coefficients for a similar expansion of the radial loading distribution $\Gamma(\eta)$. These coefficients are given by

$$H_{nk} = \int_h^1 \eta G_{nB}(nB\eta)R_{nB}(K_{nk}\eta)\,d\eta$$
$$\Gamma_{nk} = \int_h^1 \eta\Gamma(\eta)R_{nB}(K_{nk}\eta)\,d\eta \quad (3)$$

where h is the hub-to-tip radius ratio.

The wake functions themselves, obtained by a modification of Reissner's method,[4] are written out in the Appendix. Note that they vanish when $\Gamma(\eta) = \text{const} = \bar{\Gamma}$. The characteristic functions $R_{nB}(K_{nk}\eta)$ are normalized linear combinations of Bessel and Neumann functions, fully described in the Appendix to Ref. 5.

2) The parameter $\bar{\Gamma}$ is the mean loading across the span defined by

$$\bar{\Gamma} = \frac{2}{1-h^2}\int_h^1 \eta\Gamma(\eta)\,d\eta \quad (4)$$

and is proportional to the torque required to drive the rotor as well as the mean pressure rise [Eq. (51)].

3) The function ζ_l in Eq. (2) is the "saw tooth" function used by Reissner,[4] the essential properties of which are that $\partial\zeta_l/\partial\theta = 1$, $\partial\zeta_l/\partial z = -1$ everywhere, while the function itself is discontinuous by an amount $\pm 2\pi/B$ at $\zeta = \pm\pi/B, \pm 3\pi/B \ldots$.

4) The K_{nk}'s are radial eigenvalues, satisfying the condition that $R'_{nB}(K_{nk}) = R'_{nB}(hK_{nk}) = 0$ which implies the vanishing of the radial velocity component at the shroud and hub.

5) Finally, the λ_{nk}'s are axial eigenvalues and are given by

$$\lambda_{nk} = \frac{1}{\beta}\left(\frac{K_{nk}^2}{\rho_T^2} - \frac{n^2B^2M^2}{\beta^2}\right)^{1/2} \tag{5}$$

Recalling from Ref. 2 that for imaginary values of λ_{nk} to occur, $\rho_S < \rho_T$, where $\rho_S = \beta/M$ is the dimensionless radius of the sonic cylinder, it follows that in the present case, all the λ_{nk}'s are real and positive.

II. The Lifting Surface Theory

In the present theory, we attempt to construct a solution due to a distributed bound vortex system of strength $\gamma(\rho, \xi)$ distributed over the chordwise extent of the approximately helical surfaces representing the blades. Figure 1 shows the various systems of coordinates and notations used in what follows. For a lifting rotor, $\Gamma(\rho)$ and $\gamma(\rho, \xi)$ as shown are negative.

The blade leading edges are at $\theta = \pm\pi/B, \pm 3\pi/B \ldots$ with the zeroth blade leading edge at $\theta = \pi/B$. (ξ, x) are coordinates in the rotor axial direction, while $y_r \equiv r(\theta - \pi/B)$ is the peripheral distance at each radius, measured from the zeroth blade leading edge. (ξ', x') are coordinates in the local chordwise direction which is taken to be the direction of the helix of advance of the rotor, characterized by the angle $\phi = \tan^{-1}(\omega r/U) = \tan^{-1}\rho$ which it makes with the axial direction. y_r' is in the normal direction to x'.

The bound vortex distribution $\gamma(\rho, \xi)$ is to be such that at each radius, the chordwise integral gives the local circulation $\Gamma(r)$ around the blade.

Thus

$$\int_0^{C_{ax}(r)} \gamma(\rho, \xi)\frac{d\xi}{\cos\phi} = \Gamma(\rho) \tag{6}$$

This distributed vortex system is equivalent to a system of bound vortex filaments distributed along the chordwise direction, each having a varying strength in the radial direction. Each filament has its own wake, composed of trailing vortices, and whose field can be described by expressions such as Eqs. (1) and (2), provided $\Gamma(\rho)$ is replaced by $\gamma(\rho, \xi)\,d\xi/\cos\phi$, and "upstream" and "downstream" are taken to refer to positions upstream and downstream of the vortex filament in question. Equations (1) and (2) can thus be regarded as a Green's function solution, from which the field of the complete vortex system may be obtained by appropriate superposition. In doing the above superposition, the following should be noted.

1) Account must be taken of the differing axial and azimuthal position of each bound vortex filament.

2) The wake function for each bound vortex filament retains the same form as given in Ref. 2 and the Appendix, except that $\Gamma(\rho)$ is everywhere replaced by $\gamma(\eta, \xi)/\cos\phi$ inside the integrals. The functions thus also become dependent on ξ and will here be referred to as $\chi_{nB}(nB\rho, \xi) \equiv \chi_n(\eta, \xi)$.

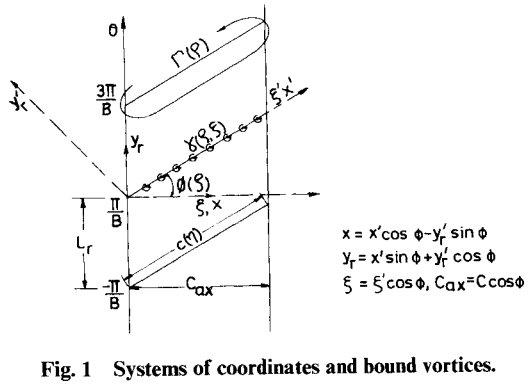

Fig. 1 Systems of coordinates and bound vortices.

3) The quantities Γ_{ok}, Γ_{nk}, H_{nk}, $\bar{\Gamma}$, Γ appearing in the Green's function solution are replaced by

$$\gamma_{ok}(\xi), \quad \gamma_{nk}(\xi), \quad \bar{\gamma}(\xi), \quad \gamma(\eta, \xi)/\cos\phi$$

where

$$\begin{aligned}
\chi_n(\eta, \xi) &= \sum_{n=1}^{\infty} h_{nk}(\xi)R_{nB}(K_{nk}\eta) \\
h_{nk}(\xi) &= \int_h^1 \eta\chi_n(\eta, \xi)R_{nB}(K_{nk}\eta)\,d\eta \\
\gamma(\eta, \xi)/\cos\phi &= \sum_{k=1}^{\infty} \gamma_{nk}(\xi)R_{nB}(K_{nk}\eta); \qquad n \neq 0 \\
&= \bar{\gamma}(\xi) + \sum_{k=1}^{\infty} \gamma_{ok}(\xi)R_0(K_{ok}\eta); \qquad n = 0 \\
\gamma_{nk}(\xi) &= \int_h^1 \eta\frac{\gamma(\eta, \xi)}{\cos\phi}R_{nB}(K_{nk}\eta)\,d\eta; \qquad n \geqq 0 \\
\bar{\gamma}(\xi) &= \frac{2}{1-h^2}\int_h^1 \frac{\gamma(\eta, \xi)}{\cos\phi}\eta\,d\eta
\end{aligned} \tag{7}$$

Note that it follows that not only the h_{nk} but all $\gamma_{ok} = 0$ when $\gamma/\cos\phi$ = constant.

We are then led to the following solution for the entire vortex system and their associated wakes.

$$\begin{aligned}
\Phi^u(\rho, z, \theta) = \frac{B}{2\pi\beta^2}\int_0^{C_{ax}} d\xi \Bigg\{ &\sum_{k=1}^{\infty} -\frac{\gamma_{ok}(\xi)}{2\lambda_{ok}} e^{\lambda_{ok}(z-\omega\xi/U)}R_0(K_{ok}\eta) + \\
&\sum_{n=1}^{\infty}\sum_{k=1}^{\infty}\left[(-1)^n\frac{h_{nk}(\xi)}{\lambda_{nk}} + \frac{i\beta^2(-1)^n}{nB}(h_{nk}(\xi)+\gamma_{nk}(\xi))\right]\times \\
&e^{inB(\theta-\omega\xi/U)}\,e^{(inBM^2/\beta^2+\lambda_{nk})(z-\omega\xi/U)}R_{nB}(K_{nk}\eta)\Bigg\} \equiv \\
&\frac{B}{2\pi\beta^2}\int_0^{C_{ax}} d\xi[\delta\Phi^u]; \qquad z \leqq 0
\end{aligned} \tag{8}$$

$$\begin{aligned}
\Phi^d(\rho, z, \theta) = \frac{B}{2\pi\beta^2}\int_0^{C_{ax}} d\xi \Bigg\{ &\bar{\gamma}(\xi)\left(z - \frac{\omega\xi}{U}\right) + \\
&\frac{\beta^2\gamma(\eta, \xi)}{\cos\phi}\zeta_l - \sum_{k=1}^{\infty}\frac{\gamma_{ok}(\xi)}{2\lambda_{ok}}e^{-\lambda_{ok}(z-\omega\xi/U)}R_0(K_{ok}\eta) + \\
&\sum_{n=1}^{\infty}\sum_{k=1}^{\infty}\frac{2i\beta^2}{nB}(-1)^n h_{nk}(\xi)\,e^{inB\zeta}R_{nB}(K_{nk}\eta) + \\
&\sum_{n=1}^{\infty}\sum_{k=1}^{\infty}\left[(-1)^n\frac{h_{nk}(\xi)}{\lambda_{nk}} - \frac{i\beta^2(-1)^n}{nB}(h_{nk}(\xi)+\gamma_{nk}(\xi))\right]\times \\
&e^{inB(\theta-\omega\xi/U)}\,e^{(inBM^2/\beta^2-\lambda_{nk})(z-\omega\xi/U)}R_{nB}(K_{nk}\eta)\Bigg\} \equiv \\
&\frac{B}{2\pi\beta^2}\int_0^{C_{ax}} d\xi[\delta\Phi^d]; \qquad z \geqq \frac{\omega c_{ax}}{U}
\end{aligned} \tag{9}$$

$$\begin{aligned}
\Phi^i(\rho, z, \theta) = \frac{B}{2\pi\beta^2}\Bigg\{\int_0^x \delta\Phi^d\,d\xi + \int_x^{C_{ax}} \delta\Phi^u\,d\xi\Bigg\}; \\
0 \leqq z \leqq \frac{\omega c_{ax}}{U}
\end{aligned} \tag{10}$$

For the sake of brevity in what follows, we shall write the coefficients $h_{nk}(\xi)$, $\gamma_{nk}(\xi)$ merely as h_{nk}, γ_{nk}, their dependence on ξ being understood. Similarly, the functions $R_0(K_{ok}\eta)$, $R_{nB}(K_{nk}\eta)$ will simply be written as R_0 and R_{nB}, respectively.

An alternative approach to the lifting surface theory, involving the use of pressure dipole representations, has recently been given by Namba.[6] In this approach, a solution for the disturbance pressure, as opposed to the velocity potential, is sought.

III. Induced Velocity Field

The axial, tangential, and radial perturbation velocities (u, v, w) are obtained, respectively, from

$$u = \frac{\omega}{U}\frac{\partial\Phi}{\partial z}, \qquad v = \frac{\omega}{\rho U}\frac{\partial\Phi}{\partial\theta}, \qquad w = \frac{\omega}{U\rho_T}\frac{\partial\Phi}{\partial\eta} \tag{11}$$

where the appropriate expression for Φ is used, depending on the region of interest. We now proceed to compare results of the present theory with actuator disk and cascade theories.

A. Relation to Axisymmetric "Through-Flow" or Actuator Disk Theories

The essential basis of the through-flow theories is that they average out the peripheral fluctuations in the flow, distributing the vorticity throughout the wake, rather than having it concentrated in individual vortex sheets. To compare the present theory, therefore, we may take the peripheral averages of the velocity profiles obtained from Eqs. (8, 9, and 11). If these averages are denoted by the symbol $\langle\ \rangle$, it is easily shown that

$$\langle u\rangle^u = -\frac{\omega B}{4\pi U\beta^2}\sum_{k=1}^{\infty}\int_0^{C_{ax}(\max)} d\xi\, e^{\lambda_{ok}(z-\omega\xi/U)}\gamma_{ok}R_0 \tag{12a}$$

$$\langle v\rangle^u = 0 \tag{12b}$$

$$\langle w\rangle^u = -\frac{\omega B}{4\pi\beta U}\sum_{k=1}^{\infty}\int_0^{C_{ax}(\max)} d\xi\, e^{\lambda_{ok}(z-\omega\xi/U)}\gamma_{ok}R_0' \tag{12c}$$

and that

$$\langle u\rangle^d = \frac{\omega B}{2\pi U\beta^2}\left\{\bar{\Gamma}-\beta^2\Gamma(\eta)+\frac{1}{2}\sum_{k=1}^{\infty}\int_0^{C_{ax}(\max)} d\xi\, e^{-\lambda_{ok}(z-\omega\xi/U)}\gamma_{ok}R_0\right. \tag{13a}$$

$$\langle v\rangle^d = B\Gamma(\eta)/2\pi r \tag{13b}$$

$$\langle w\rangle^d = -\frac{\omega B}{4\pi\beta U}\sum_{k=1}^{\infty}\int_0^{C_{ax}(\max)} d\xi\, e^{-\lambda_{ok}(z-\omega\xi/U)}\gamma_{ok}R_0' \tag{13c}$$

It is apparent from Eqs. (12c) and (13c) that the peripheral averages of the radial velocity decay nearly symmetrically about $z = 0$. For a blade of zero chord, these velocities are symmetrical about the $z = 0$ plane as in actuator disk theory, vanishing at large distance from the blade. Similarly, the peripherally averaged axial perturbation velocity decays exponentially to zero far upstream while far downstream, it varies with radius according to the relation

$$\langle u\rangle^d(z\to\infty) = \frac{\omega B}{2\pi U\beta^2}\{\bar{\Gamma}-\beta^2\Gamma(\eta)\} \equiv \frac{\tan\phi}{L_r\beta^2}(\bar{\Gamma}-\beta^2\Gamma) \tag{14}$$

where ϕ is the local freestream air angle ($\tan^{-1}\omega r/U$), and $L_r \equiv 2\pi r/B$ is the local blade spacing.

The corresponding tangential velocity is zero everywhere upstream, jumps across the blade row to $B\Gamma(r)/2\pi r$, and has that value everywhere downstream. In all the above features, the present theory is similar to the actuator disk and related theories.[1] Furthermore, the mean of the far upstream and far downstream values of $\langle u\rangle$ and $\langle v\rangle$ may be interpreted as the induced velocities in the plane of an equivalent actuator disk replacing the actual blade row. Denoting these values by $u_{ad}(0)$, $v_{ad}(0)$, respectively, we have

$$u_{ad}(0) = \frac{\tan\phi}{2L_r\beta^2}(\bar{\Gamma}-\beta^2\Gamma) \tag{15a}$$

$$v_{ad}(0) = B\Gamma(\eta)/4\pi r \tag{15b}$$

Expressed as components along and perpendicular to the chordwise direction of the blade, these may be written, after some rearrangement, as

$$u'_{ad}(0) = \frac{\Gamma\sin\phi}{2L_r\beta^2} - \frac{\sin\phi}{2L_r\beta^2}(\Gamma-\bar{\Gamma}) \tag{16a}$$

$$v'_{ad}(0) = \frac{\beta_r^2\cos\phi}{2L_r\beta^2}\Gamma + \frac{\sin^2\phi}{2L_r\beta^2\cos\phi}(\Gamma-\bar{\Gamma}) \tag{16b}$$

In the previous equations, the first term represents the contribution of the local circulation to the induced velocities in the plane of the rotor (actuator disk), while the second term, proportional to $(\Gamma-\bar{\Gamma})$, represents the contribution of the azimuthally averaged wake, and would be zero for uniform loading. An alternative interpretation of the $(\Gamma-\bar{\Gamma})$ contributions, in terms of the displacement of the mean stream surfaces, is given in Ref. 7.

As pointed out in Ref. 7, the vorticity field, $\vec{\Omega}$, defined by Eqs. (12a, b, and c), is everywhere zero, while that defined by Eqs. (13a, b, and c) is such that

$$\Omega_r = 0, \qquad \Omega_\theta = \frac{\omega}{UL_T}\Gamma'(\eta), \qquad \Omega_z = \frac{\Gamma'(\eta)}{rL_T} \tag{17}$$

Thus, the downstream vorticity vector makes with the axial direction, the angle $\tan^{-1}(\omega r/U)$, so that the net effect of defining an equivalent axisymmetric flow through averaging the more detailed three-dimensional theory is to replace the original concentrated vorticity by an equal total amount of vorticity which is however distributed uniformly over the flow annulus, yet still oriented along the zeroth-order streamlines. This feature is characteristic of the axisymmetric through-flow theories.

B. General Results for Flow within the Blade Row

We now shift attention to the flow within the blade row, as given by Eqs. (10) and (11). Here it will be more instructive to look at the velocity components (u', v') in the directions of the (x', y_r') coordinates (see Fig. 1). These velocity components are obtainable from Eq. (10) through

$$u' = \frac{\omega}{U(1+\rho^2)^{1/2}}\left(\frac{\partial\Phi^i}{\partial z}+\frac{\partial\Phi^i}{\partial\theta}\right) \tag{18}$$

$$v' = -\frac{\omega\rho}{U(1+\rho^2)^{1/2}}\left(\frac{\partial\Phi^i}{\partial z}-\frac{1}{\rho^2}\frac{\partial\Phi^i}{\partial\theta}\right) \tag{19}$$

Introducing the abbreviated notation

$$\psi \equiv \theta - \frac{\omega\xi}{U} + \frac{M^2}{\beta^2}\left(z-\frac{\omega\xi}{U}\right)$$

and carrying out the indicated operations, we obtain, for $0 \leqq z \leqq \omega c_{ax}/U$

$$\begin{aligned} u'(\eta,z,\theta) = \frac{B\omega}{4\pi\beta^2U(1+\rho^2)^{1/2}}\Bigg[&\bar{\Gamma}+\left\{\int_0^x d\xi-\int_x^{C_{ax}}d\xi\right\}\bar{\gamma}(\xi)+\\ &\sum_{k=1}^{\infty}\left\{\int_0^x d\xi\, e^{-\lambda_{ok}(z-\omega\xi/U)}-\int_x^{C_{ax}}d\xi\, e^{\lambda_{ok}(z-\omega\xi/U)}\right\}\gamma_{ok}R_0+\\ &2i\sum_{n=1}^{\infty}\sum_{k=1}^{\infty}(-1)^n\int_0^{C_{ax}}d\xi\, e^{inB\psi}e^{-\lambda_{nk}|z-\omega\xi/U|}\times\\ &\left\{\frac{\lambda_{nk}\beta^2}{nB}(\gamma_{nk}+h_{nk})+\frac{nBh_{nk}}{\beta^2\lambda_{nk}}\right\}R_{nB}+\\ &2\sum_{n=1}^{\infty}\sum_{k=1}^{\infty}(-1)^n\left\{\int_0^x d\xi\, e^{-\lambda_{nk}(z-\omega\xi/U)}-\right.\\ &\left.\left.\int_x^{C_{ax}}d\xi\, e^{\lambda_{nk}(z-\omega\xi/U)}\right\}e^{inB\psi}\gamma_{nk}R_{nB}\right] \end{aligned} \tag{20}$$

$$\begin{aligned} v'(\eta,z,\theta) = \frac{-B\omega\rho}{4\pi\beta^2U(1+\rho^2)^{1/2}}\Bigg[&\bar{\Gamma}-\beta^2\left(1+\frac{1}{\rho^2}\right)\Gamma+\\ &\left\{\int_0^x d\xi-\int_x^{C_{ax}}d\xi\right\}\left\{\bar{\gamma}(\xi)-\beta^2\left(1+\frac{1}{\rho^2}\right)\frac{\gamma(\eta,\xi)}{\cos\phi}\right\}+\\ &\sum_{k=1}^{\infty}\left\{\int_0^x d\xi\, e^{-\lambda_{ok}(z-\omega\xi/U)}-\int_x^{C_{ax}}d\xi\, e^{\lambda_{ok}(z-\omega\xi/U)}\right\}\gamma_{ok}R_0+\\ &2i\sum_{n=1}^{\infty}\sum_{k=1}^{\infty}(-1)^n\int_0^{C_{ax}}d\xi\, e^{inB\psi}e^{-\lambda_{nk}|z-\omega\xi/U|}\times\\ &\left\{\frac{\lambda_{nk}\beta^2}{nB}(\gamma_{nk}+h_{nk})+\frac{nB}{\lambda_{nk}\beta^2}\left(M^2-\frac{\beta^2}{\rho^2}\right)h_{nk}\right\}R_{nB}+\\ &2\sum_{n=1}^{\infty}\sum_{k=1}^{\infty}(-1)^n\left\{\int_0^x d\xi\, e^{-\lambda_{nk}(z-\omega\xi/U)}-\int_x^{C_{ax}}d\xi\, e^{\lambda_{nk}(z-\omega\xi/U)}\right\}\times\\ &\left\{\left(M^2-\frac{\beta^2}{\rho^2}\right)\gamma_{nk}-\beta^2\left(1+\frac{1}{\rho^2}\right)h_{nk}\right\}e^{inB\psi}R_{nB}+\\ &4\beta^2\left(1+\frac{1}{\rho^2}\right)\sum_{n=1}^{\infty}(-1)^n e^{inB\zeta}\int_0^x\chi_n(\eta,\xi)\,d\xi\Bigg] \end{aligned} \tag{21}$$

The abovementioned expressions for u' and v' are quite general and are valid for both subsonic and supersonic relative

flow. However, the qualitative character of these expressions depends strongly on whether λ_{nk} is real or imaginary, that is, on whether the relative flow is subsonic or supersonic. The subsequent analysis is therefore confined to real values of λ_{nk}, the case of supersonic relative flow being deferred to a later paper, when we shall have cause to refer to Eqs. (20) and (21) again.

C. Relation to Two-Dimensional Cascade Theory

Equations (20) and (21) can be shown to contain the two-dimensional cascade approximation to the flow over the blade at each radial section. To do this, we consider the limit as the number of blades becomes very large, and $h \to 1$. McCune[8] has shown that this limiting process leads to the appropriate quasi-two-dimensional flow at the blade tip.

We note that

$$\lim_{\substack{B\to\infty \\ h\to 1}} \lambda_{nk} = \frac{nB}{\beta^2\rho_T}(1-M_T^2)^{1/2} \equiv \frac{nB\beta_T}{\beta^2\rho_T} \tag{22}$$

and

$$\frac{\omega}{U}\lambda_{ok} = \frac{K_{ok}}{\beta r_T} = \frac{2\pi}{B}\frac{K_{ok}}{L_T\beta} \to 0 \quad \text{as} \quad B\to\infty$$

where M_T is the relative Mach number at the blade tips, and $L_T = 2\pi r_T/B$ is taken to be finite as $B \to \infty$. This suggests that, in order to obtain the quasi-two-dimensional limit at any radial section, we define a $\lambda_r{}^n$, given by

$$\lambda_r{}^n = nB\beta_r/\beta^2\rho \tag{23}$$

where $\beta_r = (1-M_r^2)^{1/2}$ and M_r is the local relative Mach number.

Of course, in order to obtain the required cascade approximation, in addition to taking the abovementioned limits, we would have to exclude also from the general solution the effect of loading variation along the span; that is, the influence of the wakes. Thus, all the terms involving the wake functions in Eqs. (20) and (21) would be excluded. When this is done, and λ_{nk} is everywhere replaced by $\lambda_r{}^n$ in the remaining terms, we obtain the appropriate quasi-two-dimensional flow about each blade section. If we denote the corresponding velocity components by u'_{2D} and v'_{2D}, and define the following:

$y_r \equiv r(\theta - \pi/B)$

$L_r \equiv 2\pi r/B$ (see Fig. 1) the local blade spacing

$$Y \equiv y_r - \xi\tan\phi + \frac{M^2}{\beta^2}(x-\xi)\tan\phi = y_r + \frac{M^2x}{\beta^2}\tan\phi - \frac{\xi}{\beta^2}\tan\phi$$

the following expressions for u'_{2D} and v'_{2D} are obtained:

$$u'_{2D}(\eta, x, y_r) = \frac{\sin\phi}{2L_r\beta^2}\bar{\Gamma} + \frac{\sin\phi}{2L_r\beta^2}\left\{\int_0^x \frac{d\xi}{\cos\phi}\gamma(\eta,\xi) - \int_x^{C_{ax}} \frac{d\xi}{\cos\phi}\gamma(\eta,\xi)\right\}\left[1+2\sum_{n=1}^{\infty} e^{2\pi n/L_r(-\beta_r/\beta^2|x-\xi|+iY)}\right] + \frac{i\beta_r\cos\phi}{2L_r\beta^2}\int_0^{C_{ax}}\frac{d\xi}{\cos\phi}\gamma(\eta,\xi)\times\left\{2\sum_{n=1}^{\infty} e^{2\pi n/L_r(-\beta_r/\beta^2|x-\xi|+iY)}+1\right\} \tag{24}$$

$$v'_{2D}(\eta, x, y_r) = -\frac{\sin^2\phi\bar{\Gamma}}{2L_r\beta^2\cos\phi} + \frac{\Gamma}{2L_r\cos\phi} + \frac{\beta_r{}^2\cos\phi}{2L_r\beta^2}\left\{\int_0^x \gamma(\eta,\xi)\frac{d\xi}{\cos\phi} - \int_x^{C_{ax}}\gamma(\eta,\xi)\frac{d\xi}{\cos\phi}\right\}\times\left[1+2\sum_{n=1}^{\infty} e^{2\pi n/L_r(-\beta_r/\beta^2|x-\xi|+iY)}\right] - \frac{i\beta_r\sin\phi}{2L_r\beta^2}\times\int_0^{C_{ax}}\gamma(\eta,\xi)\frac{d\xi}{\cos\phi}\left\{2\sum_{n=1}^{\infty} e^{2\pi n/L_r(-\beta_r/\beta^2|x-\xi|+iY)}+1\right\} \tag{25}$$

The term 1 in the last bracket of either Eq. (24) or Eq. (25) has been added merely for convenience. It does not affect the final results as it adds only a purely imaginary term, while only the real parts of the expressions are needed. It however facilitates further simplification of these results. If we note that β_r is real and positive, recall the identity

$$\coth z = -\left(1+2\sum_{n=1}^{\infty} e^{2nz}\right); \qquad Re(z) < 0 \tag{26}$$

and use the symmetry property of $\coth z$ with respect to the real part of z, namely

$$\text{Real}\,[\coth(-x+iy)] = -\text{Real}\,[\coth(x+iy)] \tag{27}$$

we may express Eqs. (24) and (25) more simply as

$$u'_{2D}(\eta, x, y_r) = \frac{\sin\phi}{2L_r\beta^2}\bar{\Gamma} + \frac{(\sin\phi - i\beta_r\cos\phi)}{2L_r\beta^2}\times\int_0^{C_{ax}}\frac{d\xi}{\cos\phi}\gamma(\eta,\xi)\coth\frac{\pi}{L_r}\left[\frac{\beta_r}{\beta^2}(x-\xi)+iY\right] \tag{28}$$

$$v'_{2D}(\eta, x, y_r) = -\frac{\sin^2\phi\bar{\Gamma}}{2L_r\beta^2\cos\phi} + \frac{\Gamma}{2L_r\cos\phi} + \frac{\beta_r(\beta_r\cos\phi + i\sin\phi)}{2L_r\beta^2}\int_0^{C_{ax}}\frac{d\xi}{\cos\phi}\times\gamma(\eta,\xi)\coth\frac{\pi}{L_r}\left[\frac{\beta_r}{\beta^2}(x-\xi)+iY\right] \tag{29}$$

It will be even more convenient, for purposes of identifying the two-dimensional cascade results, to express the above velocity components in the variables (η, x', y_r') as shown in Fig. 1. It is easily shown that

$$u'_{2D}(\eta, x', y_r') = \frac{\Gamma\sin\phi}{2L_r\beta^2} - \frac{\sin\phi}{2L_r\beta^2}(\Gamma-\bar{\Gamma}) - \frac{i(\beta_r\cos\phi + i\sin\phi)}{2L_r\beta^2}\int_0^C d\xi'\gamma(\eta,\xi')\times\coth\left\{\frac{\pi}{L_r\beta^2}(\beta_r\cos\phi + i\sin\phi)[(x'-\xi')+iy_r'\beta_r]\right\} \tag{30}$$

$$v'_{2D}(\eta, x', y_r') = \frac{\beta_r{}^2\cos\phi\Gamma}{2L_r\beta^2} + \frac{\sin^2\phi}{2L_r\beta^2\cos\phi}(\Gamma-\bar{\Gamma}) + \frac{\beta_r(\beta_r\cos\phi + i\sin\phi)}{2L_r\beta^2}\int_0^C d\xi'\gamma(\eta,\xi')\times\coth\left\{\frac{\pi}{L_r\beta^2}(\beta_r\cos\phi + i\sin\phi)[(x'-\xi')+iy_r'\beta_r]\right\} \tag{31}$$

Comparison of the expressions with Eqs. (16a) and (16b) shows that the first two terms of Eq. (30) represent the local induced u' velocity component at the blade by an equivalent actuator disk replacing the actual blade row, while the first two terms of Eq. (31) have a similar interpretation. These terms represent a modification of the original basic flow by the axially symmetric stream surfaces of the peripherally averaged flow, and to these must be added the induced velocities of the potential vane flow through the "cascades" representing the blade passages. The latter is represented by the terms involving the chordwise integrals in Eqs. (30) and (31) and give the contribution of the detailed blade chordwise loading to the local quasi-two-dimensional flow. These terms can be reduced to the standard result for an equivalent incompressible cascade flow[9,10] by use of the Prandtl-Glauert-Göthert transformation. Because of our approximate treatment of the terms in Eqs. (20) and (21) involving $e^{\pm\lambda_{ok}(z-\omega\xi/U)}$, Eqs. (30) and (31) are limited to regions within and near the blade row, $x'/L_r < 1$. The cascade results cannot reproduce the actual three-dimensional total turning angle,[2] which can be obtained from Eq. (16b).

We note that for uniform loading ($\Gamma = \bar{\Gamma}$), Eq. (31) vanishes at the sonic radius, i.e., at the radius where $M_r = 1$, for all values of y_r', thus exhibiting the characteristic two-dimensional transonic degeneracy. This degeneracy however is removed when the complete three-dimensional results are considered.

Further, Eq. (30) contains the required local discontinuity in the u' velocity component at the blade surface, while Eq. (31) is continuous there. To show this, we note that $\coth z$ has a first

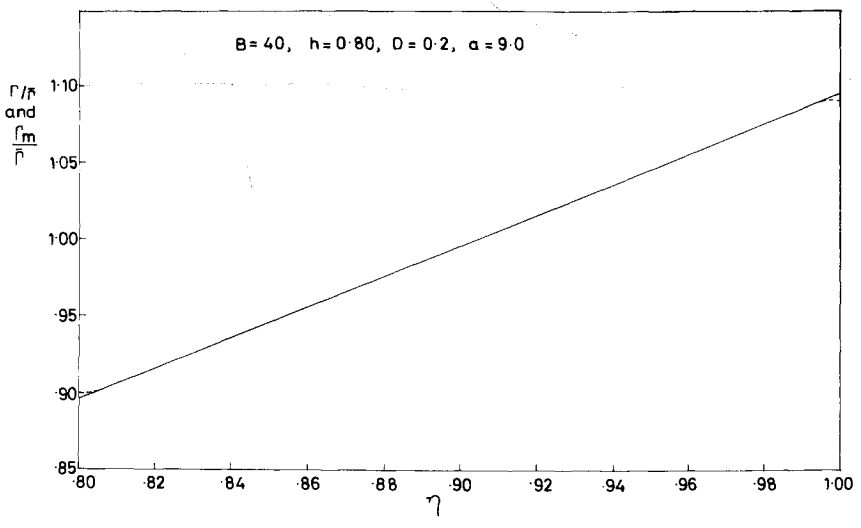

Fig. 2 Purely linear loading [Eq. (48)] compared with modified linear loading [Eq. (49)].

order pole at $z = 0$, but is regular for $|z| > 0$. Thus, a Laurent series expansion has the form

$$\coth z = \frac{1}{z} + \sum_{n=1}^{\infty} a_n z^n \tag{32}$$

Introducing this into Eq. (30), and stopping at the first term of the expansion, we obtain

$$u'_{2D}(\eta, x', y_r') = \frac{\sin\phi\bar{\Gamma}}{2L_r\beta^2} - \frac{i}{2\pi}\int_0^C d\xi'\gamma(\eta,\xi')\frac{(x'-\xi')-iy_r'\beta_r}{(x'-\xi')^2+\beta_r^2 y_r'^2} + \text{regular terms} \tag{33}$$

Thus

$$\lim_{y_r'\to 0\pm} Re\,(u'_{2D}) = \frac{\sin\phi}{2L_r\beta^2}\bar{\Gamma} - \frac{1}{2\pi}\int_0^C d\xi'\gamma(\eta,\xi') \times \lim_{y_r'\to 0\pm}\left[\frac{y_r'\beta_r}{(x'-\xi')^2+\beta_r^2 y_r'^2}\right] + \text{regular terms} \tag{34}$$

But

$$\frac{1}{\pi}\lim_{y_r'\to 0\pm}\left[\frac{y_r'\beta_r}{(x'-\xi')^2+\beta_r^2 y_r'^2}\right] = \pm\delta(x'-\xi') \tag{35}$$

Hence

$$u'_{2D}(\eta, x', y_r' = 0+) = \frac{\sin\phi}{2L_r\beta^2}\bar{\Gamma} - \tfrac{1}{2}\gamma(\eta, x') + \text{regular terms}$$

and

$$u'_{2D}(\eta, x', y_r' = 0-) = \frac{\sin\phi}{2L_r\beta^2}\bar{\Gamma} + \tfrac{1}{2}\gamma(\eta, x') + \text{regular terms}$$

so that the jump in u'_{2D} across the blade, $\Delta u'_{2D}$ is given by

$$\Delta u'_{2D}(\eta, x') = -\gamma(\eta, x') \tag{36}$$

A similar analysis shows that v'_{2D} is continuous across the blade row.

D. Finite Blade and Wake Effects

The remaining expression from the general results [Eqs. (20) and (21)] which are left after extracting the local quasi-two-dimensional flow [Eqs. (24) and (25)] may be regarded as three-dimensional corrections to cascade through-flow theory, and the corresponding velocity components denoted by u'_{3D} and v'_{3D}.

Thus

$$\begin{aligned} u'_{3D}(\eta, z, \theta) &\equiv u'(\eta, z, \theta) - u'_{2D}(\eta, z, \theta) \\ v'_{3D}(\eta, z, \theta) &\equiv v'(\eta, z, \theta) - v'_{2D}(\eta, z, \theta) \end{aligned} \tag{37}$$

These expressions may conveniently be written out in terms of the following operators:

$$I_1(x,\xi) = \sum_{k=1}^{\infty}\left\{\int_0^x d\xi(e^{-\lambda_{ok}(z-\omega\xi/U)} - 1) - \int_x^{C_{ax}} d\xi(e^{\lambda_{ok}(z-\omega\xi/U)} - 1)\right\}$$

$$I_2(x,\xi) = \sum_{n=1}^{\infty}\sum_{k=1}^{\infty}\left\{\int_0^x d\xi[e^{-\lambda_{nk}(z-\omega\xi/U)} - e^{-\lambda_r n(z-\omega\xi/U)}] - \int_x^{C_{ax}} d\xi[e^{\lambda_{nk}(z-\omega\xi/U)} - e^{\lambda_r n(z-\omega\xi/U)}]\right\} \tag{38}$$

$$I_3(x,\xi) = \sum_{n=1}^{\infty}\sum_{k=1}^{\infty}\int_0^{C_{ax}} d\xi(\lambda_{nk}\,e^{-\lambda_{nk}|z-\omega\xi/U|} - \lambda_r{}^n\,e^{-\lambda_r n|z-\omega\xi/U|})$$

Thus, the three-dimensional corrections take the form

$$u'_{3D} = \frac{B\omega}{4\pi\beta^2 U(1+\rho^2)^{1/2}}\Bigg[I_1(x,\xi)\gamma_{ok}R_0 + 2I_2(x,\xi)\gamma_{nk}R_{nB}\,e^{inB(\psi+\pi/B)} + 2iI_3(x,\xi)\frac{\beta^2}{nB}\gamma_{nk}R_{nB}\,e^{inB(\psi+\pi/B)} + 2i\sum_{n=1}^{\infty}\sum_{k=1}^{\infty}\int_0^{C_{ax}} d\xi\left(\frac{nB}{\beta^2\lambda_{nk}} + \frac{\beta^2\lambda_{nk}}{nB}\right)h_{nk}R_{nB} \times e^{inB(\psi+\pi/B)}\,e^{-\lambda_{nk}|z-\omega\xi/U|}\Bigg] \tag{39}$$

$$v'_{3D} = \frac{-B\omega\rho}{4\pi\beta^2 U(1+\rho^2)^{1/2}}\Bigg[I_1(x,\xi)\gamma_{ok}R_0 - \frac{2\beta_r{}^2\cos^2\phi}{\sin^2\phi}I_2(x,\xi)\,e^{inB(\psi+\pi/B)}\gamma_{nk}R_{nB} + 2iI_3(x,\xi)\frac{\beta^2}{nB}\gamma_{nk}R_{nB}\,e^{inB(\psi+\pi/B)} + \frac{4\beta^2}{\sin^2\phi}\sum_{n=1}^{\infty}(-1)^n e^{inB\zeta}\int_0^x \chi_n(\eta,\xi)\,d\xi - \frac{2\beta^2}{\sin^2\phi}\sum_{n=1}^{\infty}\sum_{k=1}^{\infty}\left\{\int_0^x d\xi\,e^{-\lambda_{nk}(z-\omega\xi/U)} - \int_x^{C_{ax}} d\xi\,e^{\lambda_{nk}(z-\omega\xi/U)}\right\}e^{inB(\psi+\pi/B)}h_{nk}R_{nB} + 2i\sum_{n=1}^{\infty}\sum_{k=1}^{\infty}\int_0^{C_{ax}} d\xi\left[\frac{nB}{\lambda_{nk}}\left(\frac{M^2}{\beta^2} - \frac{1}{\rho^2}\right) + \frac{\lambda_{nk}\beta^2}{nB}\right]\times e^{inB(\psi+\pi/B)}\,e^{-\lambda_{nk}|z-\omega\xi/U|}h_{nk}R_{nB}\Bigg] \tag{40}$$

These corrections are of two types; namely those due to the number of blades being finite, and those due to the effect of trailing vortices. In Eqs. (39) and (40), for regions near the blade

row (z/ρ_T not too large), the terms involving the operators would vanish as $\lambda_{nk} \to \lambda_r{}^n$, $\lambda_{ok} \to 0$; that is as $B \to \infty$. Hence these terms may be said to represent the finite blade effects. The other terms would vanish if $\Gamma'(r) = 0$ since then, both the wake function and the h_{nk}'s vanish. These then represent the effects of the wakes of the individual trailing vortices behind the blades.

The expressions for the three-dimensional corrections, as given by Eqs. (39) and (40) are quite general. For computational purposes, it is helpful to make the assumption that the loading function $(1/\cos\phi)\gamma(\eta, \xi)$ is separable in η and ξ, so that it may be written as

$$\frac{1}{\cos\phi}\gamma(\eta, \xi) = \Gamma(\eta)g(\xi) \tag{41}$$

where $g(\xi)$ represents a chordwise loading function. If further, we assume that $c_{ax} = \text{const}$, then the loading function satisfies the condition that

$$\int_0^{C_{ax}} g(\xi)\, d\xi = 1 \tag{42}$$

Equation (41) enables the quantities $\gamma_{nk}(\xi)$, $\bar{\gamma}(\xi)$, $\chi_n(\eta, \xi)$, and $h_{nk}(\xi)$ to be expressed in terms of the corresponding lifting line quantities, namely

$$\begin{aligned} \gamma_{nk}(\xi) &= g(\xi)\Gamma_{nk}, \qquad n \geqq 0 \\ \bar{\gamma}(\xi) &= g(\xi)\bar{\Gamma} \\ \chi_n(\eta, \xi) &= g(\xi)G_{nB}(nB\eta\rho_T) \\ h_{nk}(\xi) &= g(\xi)H_{nk} \end{aligned} \tag{43}$$

Using the previous simplifications, and substituting $\theta = z + \pi/B$ in the general expressions, we obtain the following expressions for the three-dimensional corrections at the blade surface:

$$\begin{aligned} u'_{3D}(\eta, x', y_r' = 0) = \frac{\sin\phi}{2L_r\beta^2}\Bigg\{ & \sum_{k=1}^{\infty}[S_{ok}{}^{(1)}(\rho, z) - S_{ok}{}^{(2)}(\rho, z)]\Gamma_{ok}R_0 + \\ & 2\sum_{n=1}^{\infty}\sum_{k=1}^{\infty}[S_{nk}{}^{(1)}(\rho, z) - S_{nk}{}^{(2)}(\rho, z)]\Gamma_{nk}R_{nB} + \\ & 2i\sum_{n=1}^{\infty}\sum_{k=1}^{\infty}\frac{\beta^2}{nB}S_{nk}{}^{(3)}(\rho, z)\Gamma_{nk}R_{nB} + \\ & 2i\sum_{n=1}^{\infty}\sum_{k=1}^{\infty}\left(\frac{nB}{\beta^2\lambda_{nk}} + \frac{\lambda_{nk}\beta^2}{nB}\right)S_{nk}{}^{(4)}(\rho, z)H_{nk}R_{nB}\Bigg\} \end{aligned} \tag{44}$$

$$\begin{aligned} v'_{3D}(\eta, x', y_r' = 0) = -\frac{\sin^2\phi}{2L_r\beta^2\cos\phi}\Bigg\{ & \sum_{k=1}^{\infty}[S_{ok}{}^{(1)}(\rho, z) - \\ & S_{ok}{}^{(2)}(\rho, z)]\Gamma_{ok}R_0 - \frac{2\beta_r{}^2\cos^2\phi}{\sin^2\phi}\sum_{n=1}^{\infty}\sum_{k=1}^{\infty}[S_{nk}{}^{(1)}(\rho, z) - \\ & S_{nk}{}^{(2)}(\rho, z)]\Gamma_{nk}R_{nB} + 2i\sum_{n=1}^{\infty}\sum_{k=1}^{\infty}\frac{\beta^2}{nB}S_{nk}{}^{(3)}(\rho, z)\Gamma_{nk}R_{nB} + \\ & 2i\sum_{n=1}^{\infty}\sum_{k=1}^{\infty}\left[\frac{nB}{\lambda_{nk}}\left(\frac{M^2}{\beta^2} - \frac{1}{\rho^2}\right) + \frac{\lambda_{nk}\beta^2}{nB}\right]S_{nk}{}^{(4)}(\rho, z)H_{nk}R_{nB} - \\ & \frac{2\beta^2}{\sin^2\phi}\sum_{n=1}^{\infty}\sum_{k=1}^{\infty}[S_{nk}{}^{(5)} - S_{nk}{}^{(6)}]H_{nk}R_{nB} + \\ & \frac{4\beta^2}{\sin^2\phi}S_D(\rho, z)\sum_{n=1}^{\infty}G_n(\eta\rho_T)\Bigg\} \end{aligned} \tag{45}$$

where, with $\lambda_r{}^0 \equiv 0$, the S_{nk} functions are given by

$$S_{nk}{}^{(1)}(\rho, z) = \int_0^x \frac{1}{\cos\phi}d\xi\left[e^{-\lambda_{nk}(z-\omega\xi/U)} - e^{-\lambda_r{}^n(z-\omega\xi/U)}\right] \times g(\xi)\, e^{inB\omega/U\beta^2(x-\xi)}, \qquad n \geqq 0$$

$$S_{nk}{}^{(2)}(\rho, z) = \int_x^{C_{ax}} \frac{1}{\cos\phi}d\xi\left[e^{\lambda_{nk}(z-\omega\xi/U)} - e^{\lambda_r{}^n(z-\omega\xi/U)}\right] \times g(\xi)\, e^{inB\omega/U\beta^2(x-\xi)}, \qquad n \geqq 0$$

$$S_{nk}{}^{(3)}(\rho, z) = \int_0^{C_{ax}} \frac{1}{\cos\phi}d\xi\left[\lambda_{nk}\, e^{-\lambda_{nk}|z-\omega\xi/U|} - \lambda_r{}^n\, e^{-\lambda_r{}^n|z-\omega\xi/U|}\right] \times g(\xi)\, e^{inB\omega/U\beta^2(x-\xi)}$$

$$S_{nk}{}^{(4)}(\rho, z) = \int_0^{C_{ax}} \frac{1}{\cos\phi}d\xi\, e^{-\lambda_{nk}|z-\omega\xi/U|}g(\xi)\, e^{inB\omega/U\beta^2(x-\xi)} \tag{46}$$

$$S_{nk}{}^{(5)}(\rho, z) = \int_0^x \frac{d\xi}{\cos\phi}e^{-\lambda_{nk}(z-\omega\xi/U)}g(\xi)\, e^{inB\omega/U\beta^2(x-\xi)}$$

$$S_{nk}{}^{(6)}(\rho, z) = \int_x^{C_{ax}} \frac{d\xi}{\cos\phi}e^{\lambda_{nk}(z-\omega\xi/U)}g(\xi)\, e^{inB\omega/U\beta^2(x-\xi)}$$

$$S_D(\rho, z) = \int_0^x g(\xi)\frac{d\xi}{\cos\phi}$$

This completes the determination of the three-dimensional corrections for the special case of the loading conforming to Eq. (41).

It is to be noted that for the kind of loading satisfying Eqs. (41–43), both Eqs. (21) and (45) contain terms involving the infinite summation

$$\sum_{n=1}^{\infty} G_{nB}(nB\rho)$$

An approximate expression for this infinite sum, for a large number of blades ($B \gtrsim 10$), has been given by McCune and Dharwadkar,[11] and is given in the Appendix. It is apparent from this expression that this sum is singular at the root and tip, unless $d\Gamma/d\rho$ vanishes at these points. We must therefore make a choice of $\Gamma(\rho)$ that in general satisfies these conditions. This, however, is not a serious practical limitation on the allowable choice of $\Gamma(\rho)$, since even for a choice of $\Gamma(\rho)$ that does not have vanishing derivatives at the hub and shroud, a modified $\Gamma(\rho)$ can usually be found that is indistinguishable from the actual $\Gamma(\rho)$ everywhere except at the hub and shroud, and that meets the requirements of vanishing derivatives at these points. An example is illustrated in the numerical computations.

IV. Numerical Results

In all of the results presented, we limit ourselves to the indirect or design problem. The direct problem has been treated by Namba,[6] and can also be treated by an extension of the methods of this paper, along the lines given in Ref. 11 for the lifting line approximation. The bound vortex distribution for the results presented here is assumed to satisfy Eq. (41). A chordwise loading function of the form

$$g(\xi) = \frac{1}{\pi/8c_{ax}}[\xi^*(1-\xi^*)]^{1/2} \tag{47}$$

has also been assumed where $\xi^* = \xi/c_{ax}$ and the factor ensures that Eq. (42) is satisfied.

Suppose we have as a specified loading, the linear distribution represented by

$$\Gamma(\eta)/\bar{\Gamma} = 1 - \frac{2D(1+h+h^2)}{3(1-h^2)} + \frac{D}{1-h}\eta \tag{48}$$

where the parameter D is the fractional deviation of the loading from uniformity, expressed as

$$D = (\Gamma_T - \Gamma_H)/\bar{\Gamma}$$

so that for $D = 0$, we have a uniformly loaded rotor. Equation (48) as it stands does not meet the requirements of vanishing derivatives at the hub and shroud unless $D = 0$. However, if we consider the modified loading $\Gamma_m(\eta)$ given by

$$\frac{\Gamma_m(\eta)}{\bar{\Gamma}} = 1 - \frac{2D(1+h+h^2)}{3(1-h^2)} + \frac{D}{1-h}\eta + \frac{D}{1-h}\left\{\frac{\cosh[aB(1-\eta)] - \cosh[aB(\eta-h)]}{aB\sinh[aB(1-h)]}\right\} \tag{49}$$

we find that $\Gamma_m' = 0$ at $\eta = h$ and $\eta = 1$ for all values of a. The value of a can now be chosen so as to make the last term of Eq. (49) exponentially small over the whole span, and thus nearly identical with Eq. (48).

Two cases will be considered, corresponding to $D = 0$ and $D = 0.2$ in Eq. (48). In the latter case, Eq. (49) will be used, with $a = 9.0$. A comparison of the resulting loading with that given

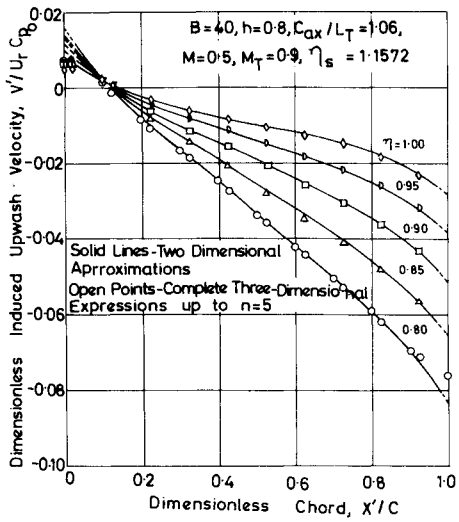

Fig. 3 Upwash velocities: local quasi-two-dimensional approximations compared with complete three-dimensional results. Uniform loading ($D = 0$).

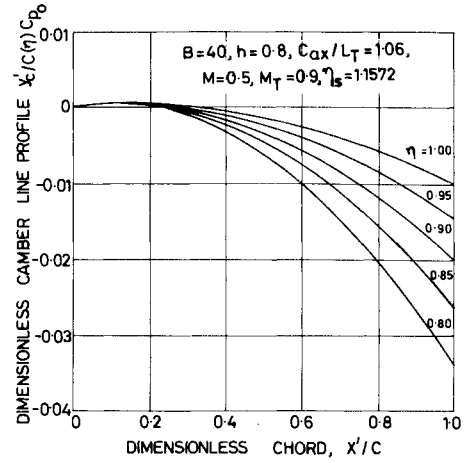

Fig. 4 Camber-line profiles for uniformly loaded blade ($D = 0$).

by Eq. (48) is shown in Fig. 2, for the geometrical parameters $B = 40$, $h = 0.8$.

The coefficients H_{nk}, Γ_{nk}, and the wake function $G_n(\eta\rho_T)$ occurring in the double series in the preceding results are fully discussed in Ref. 5. In the same reference, the convergence characteristics of the series, as well as practical guides to numerical computation of results are discussed. In general, sufficient accuracy, with an error of the order of 5%, can be expected by considering only the sum from $n = 1$ to $n = 5$. For each n, the number of terms in k would vary, becoming large as n increases. For each n the summation over k in the numerical computations was terminated at $k = k_{\max}(n)$ where $k_{\max}(n)$ for $n = 0$ to 10, are, respectively, 5, 5, 7, 9, 11, 13, 14, 15, 16, 17, and 18.

The upwash velocity on the blade surface, as given by the quasi-two-dimensional approximation, is obtained by simply setting $y_r' = 0$ in Eq. (31) while the three-dimensional corrections (finite blade-wake effects) are obtained from Eq. (45). The complete expression for the upwash, Eq. (21) is also easily expressed in terms of the S_{nk} functions of Eq. (46), and this can be used directly, when desired.

A rotor with 40 blades, a hub-tip ratio of 0.8, and a solidity, $c_{ax}/L_T = 1.06$ will be assumed in all calculations. Here $L_T = 2\pi r_T/B$ is the blade spacing at the tip. Unless otherwise indicated, the axial Mach number is taken as 0.5, and the relative tip Mach number M_T is 0.9.

It will be convenient to normalize both the upwash velocity and the camberline profile coordinates by means of the mean pressure rise coefficient C_{p0} across the blade row. Thus C_{p0}, or equivalently, the mean loading $\bar{\Gamma}/UL_T$, may be specified for the blade row consistent with the linearizing assumptions of the theory.

Noting that the perturbation pressure at any point in the flowfield is

$$\hat{p} \equiv p - \langle p_{-\infty} \rangle = -\omega\sigma_{-\infty}\left(\frac{\partial\Phi}{\partial z} + \frac{\partial\Phi}{\partial\theta}\right) \tag{50}$$

where $\sigma_{-\infty}$ is the unperturbed density far upstream of the rotor, we may differentiate the expressions for Φ upstream and downstream of the rotor, and show that

$$C_{p0} \equiv (\langle p_{+\infty} \rangle - \langle p_{-\infty} \rangle)/(\sigma_{-\infty} U^2/2) = -\frac{2\rho_T}{\beta^2}(\bar{\Gamma}/UL_T) \tag{51}$$

Case 1: Wakeless Flow

This is the case when Γ is independent of radius, and corresponds to uniform work at all radii. The wake terms are proportional to $\Gamma'(r)$, and hence are identically zero. The flow is thus everywhere the same as the local quasi-two-dimensional approximation, except for finite-blade effects. (Three-dimensional effects as used in the present discussion will refer only to the finite blade and wake effects, the local induced flow due to the equivalent actuator disk being already included in the local quasi-two-dimensional approximation to the actual flow.)

Figure 3 shows the induced upwash velocity at the blade as computed from the quasi-two-dimensional approximation, compared with results from the complete three-dimensional expressions. In the figures, $U_r = (U^2 + \omega^2 r^2)^{1/2}$ is the relative velocity at the blade section. The near coincidence of the two curves shows that finite blade effects are negligible, except perhaps near the leading and trailing edges of the blade row. It is unlikely that this effect will become significant for any practical blade configuration, as long as the loading is uniform. For this type of loading, the quasi-two-dimensional approximations to the flow are thus adequate and there is no need to use the more involved three-dimensional expressions.

The camber-line profiles corresponding to the upwash velocities of Fig. 3 are shown in Fig. 4. These are obtained by integration of the camber-line slope $v'(x', 0)/U_r$ along the chord. Thus if y_c' is the y_r' coordinate of the camber line, then

$$dy_c'/dx' = v'(x', 0)/U_r \tag{52}$$

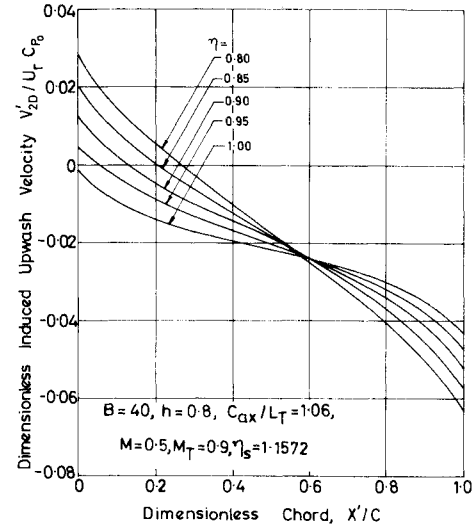

Fig. 5 Upwash velocities: quasi-two-dimensional approximations. Non-uniform loading ($D = 0.2$).

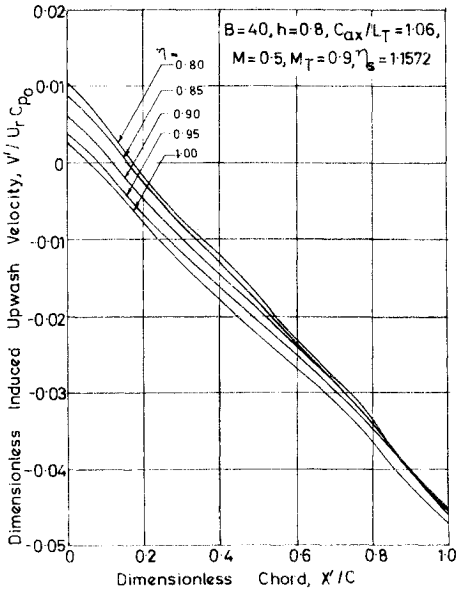

Fig. 6 Upwash velocities: complete three-dimensional results. Nonuniform loading ($D = 0.2$).

and

$$y_c'(x')/c(\eta)C_{p0} = \int_0^{x^+} \frac{v'(x',0)}{U_r C_{p0}} dx^+ \tag{53}$$

where $x^+ = x'/c$, and it is assumed that $y_c'(0) = 0$. The blade is seen to be heavily cambered at the root, becoming less cambered towards the tip.

Case 2: Wake Flow

To illustrate the influence of the wake, we consider a loading distribution such that $D = 0.2$, but with $\bar{\Gamma}/UL_T$ remaining the same as for Case 1. Figure 5 shows the two-dimensional approximations to the upwash for this case, while Fig. 6 gives the complete upwash velocities, including three-dimensional corrections. Thus, departures from the quasi-two-dimensional flow are quite significant, although even here, the 2-D approximations fairly accurately predict the upwash velocity at midchord, at all radial stations. At the root sections, its predictions are too high near the leading edge and too low near the trailing edge. The opposite is true at the tip sections. The corresponding camber-line profiles are shown in Fig. 7. The blade is now more cambered at the tip, and the variation in camber from root to tip is less than in the uniform loading case.

It thus appears that in cases where the relative Mach number at the blades is everywhere subsonic, inviscid three-dimensional effects (defined as corrections to cascade theory combined with axisymmetric through-flow theory) are almost exclusively due to the wake. For a uniformly loaded rotor, this effect is unimportant, since the wake is absent, but becomes quite significant even for moderate departures from uniform loading. The above conclusions are not necessarily valid when the relative Mach number at the tip becomes supersonic.

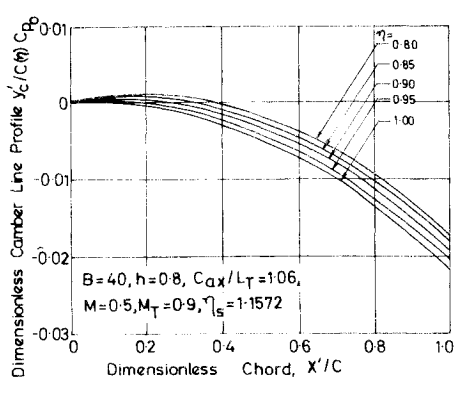

Fig. 7 Camber-line profiles for nonuniformly loaded blade ($D = 0.2$).

Appendix: Wake Functions $G_{nB}(nB\rho)$

The expression for each wake function $G_{nB}(nB\rho)$ is given in Ref. 2 as

$$G_n(\rho) \equiv G_{nB}(nB\rho) = \frac{K'(\rho_T)I'(\rho_H)K(\rho) - K'(\rho_T)K'(\rho_H)I(\rho)}{K'(\rho_T)I'(\rho_H) - K'(\rho_H)I'(\rho_T)} \times \int_{\rho_H}^{\rho_T} \hat{\rho}\, d\hat{\rho} I'(\hat{\rho}) \frac{d\Gamma}{d\hat{\rho}} + \frac{I'(\rho_T)K'(\rho_H)I(\rho) - I'(\rho_H)I'(\rho_T)K(\rho)}{K'(\rho_T)I'(\rho_H) - K'(\rho_H)I'(\rho_T)} \times \int_{\rho_H}^{\rho_T} \hat{\rho}\, d\hat{\rho} K'(\hat{\rho}) \frac{d\Gamma}{d\hat{\rho}} + I(\rho) \int_{\rho_H}^{\rho} K'(\hat{\rho})\hat{\rho} \frac{d\Gamma}{d\hat{\rho}} d\hat{\rho} - K(\rho) \int_{\rho_H}^{\rho} I'(\hat{\rho}) \frac{d\Gamma}{d\hat{\rho}} d\hat{\rho} \tag{A1}$$

where $I(\rho) \equiv I_{nB}(nB\rho)$, $K(\rho) \equiv K_{nB}(nB\rho)$ are the modified Bessel functions of the first and second kind, and $I'(\rho) \equiv (d/d\rho)I_{nB}(nB\rho)$, $K'(\rho) \equiv (d/d\rho)K_{nB}(nB\rho)$, etc. For uniform loading, $d\Gamma/d\rho = 0$, and the wake functions vanish identically. Moreover, the functions satisfy the wall boundary conditions, whether or not $d\Gamma/d\rho = 0$ at ρ_H and ρ_T.

For a large number of blades, $B \gtrsim 10$, McCune and Dharwadkar[11] have shown that the infinite sum of the wake functions,

$$\sum_{n=1}^{\infty} G_n(\rho)$$

is given by

$$\sum_{n=1}^{\infty} G_{nB}(nB\rho) \equiv \sum_{n=1}^{\infty} G_n(\rho) \approx -\frac{1}{2}\int_{\rho_H}^{\rho_T} d\hat{\rho} \left(\frac{\hat{\tau}}{\tau}\right)^{1/2} \frac{d\Gamma}{d\hat{\rho}} \times \frac{\left(\frac{\tau_T+1}{\tau_T-1}\right)^B \left(\frac{\tau-1}{\tau+1}\right)^{B/2} \left(\frac{\hat{\tau}-1}{\hat{\tau}+1}\right)^{B/2} e^{-2B[\tau_T-(\tau+\hat{\tau})/2]}}{1-\left(\frac{\tau_T+1}{\tau_T-1}\right)^B \left(\frac{\tau-1}{\tau+1}\right)^{B/2} \left(\frac{\hat{\tau}-1}{\hat{\tau}+1}\right)^{B/2} e^{-2B[\tau_T-(\tau+\hat{\tau})/2]}} + \frac{1}{2}\int_{\rho_H}^{\rho_T} d\hat{\rho} \left(\frac{\hat{\tau}}{\tau}\right)^{1/2} \frac{d\Gamma}{d\hat{\rho}} \times \frac{\left(\frac{\tau_H-1}{\tau_H+1}\right)^B \left(\frac{\tau+1}{\tau-1}\right)^{B/2} \left(\frac{\hat{\tau}+1}{\hat{\tau}-1}\right)^{B/2} e^{-2B[(\tau+\hat{\tau})/2-\tau_H]}}{1-\left(\frac{\tau_H-1}{\tau_H+1}\right)^B \left(\frac{\tau+1}{\tau-1}\right)^{B/2} \left(\frac{\hat{\tau}+1}{\hat{\tau}-1}\right)^{B/2} e^{-2B[(\tau+\hat{\tau})/2-\tau_H]}} + \frac{1}{2}\int_{\rho}^{\rho_T} d\hat{\rho} \left(\frac{\hat{\tau}}{\tau}\right)^{1/2} \frac{d\Gamma}{d\hat{\rho}} \times \frac{\left(\frac{\tau-1}{\tau+1}\right)^{B/2} \left(\frac{\hat{\tau}+1}{\hat{\tau}-1}\right)^{B/2} e^{B(\tau-\hat{\tau})}}{1-\left(\frac{\tau-1}{\tau+1}\right)^{B/2} \left(\frac{\hat{\tau}+1}{\hat{\tau}-1}\right)^{B/2} e^{B(\tau-\hat{\tau})}} - \frac{1}{2}\int_{\rho_H}^{\rho} d\hat{\rho} \left(\frac{\hat{\tau}}{\tau}\right)^{1/2} \frac{d\Gamma}{d\hat{\rho}} \times \frac{\left(\frac{\tau+1}{\tau-1}\right)^{B/2} \left(\frac{\hat{\tau}-1}{\hat{\tau}+1}\right)^{B/2} e^{-B(\tau-\hat{\tau})}}{1-\left(\frac{\tau+1}{\tau-1}\right)^{B/2} \left(\frac{\hat{\tau}-1}{\hat{\tau}+1}\right)^{B/2} e^{-B(\tau-\hat{\tau})}} \tag{A2}$$

where $\tau = (1+\rho^2)^{1/2}$.

It is obvious that the abovementioned sum is singular at $\rho = \rho_H$ and $\rho = \rho_T$ unless $d\Gamma/d\rho$ is zero at these points. Thus, the load distribution $\Gamma(\rho)$ must be selected to satisfy these conditions.

References

[1] Marble, F. E., "Three-Dimensional Flow in Turbomachines," *Princeton Series on High Speed Aerodynamics and Jet Propulsion*, Vol. 10, Princeton Univ. Press, Princeton, N.J., 1964, Sec. C, pp. 83–166.

[2] Okurounmu, O. and McCune, J. E., "Three-Dimensional Vortex

Theory of Axial Compressor Blade Rows at Subsonic and Transonic Speeds," *AIAA Journal*, Vol. 8, No. 7, July 1970, pp. 1275–1283.

[3] Goldstein, S., "On the Vortex Theory of Screw Propellers," *Proceedings of the Royal Society of London*, Ser. A, Vol. 123, No. 792, April 6, 1929, pp. 440–465.

[4] Reissner, H., "On the Vortex Theory of the Screw Propeller," *Journal of the Aeronautical Sciences*, Vol. 5, No. 1, Nov. 1937, pp. 1–7.

[5] Okurounmu, O. and McCune, J. E., "Transonic Lifting Surface Theory for Axial Compressors," K213580-1, March 1971, United Aircraft Research Labs., East Hartford, Conn.

[6] Namba, M., "Small Disturbance Theory of Rotating Subsonic and Transonic Cascades," presented at the First International Symposium on Air Breathing Engines, Marseilles, France, June 19–23, 1972.

[7] McCune, J. E. and Okurounmu, O., "Three-Dimensional Flow in Transonic Axial Compressor Blade Rows," presented at the International Symposium on the Fluid Mechanics and Design of Turbomachinery, Pennsylvania State Univ., University Park, Pa., Aug. 1970.

[8] McCune, J. E., "Three-Dimensional Theory of Axial Compressor Blade Rows—Application to Subsonic and Supersonic Flows," *Journal of the Aerospace Sciences*, Vol. 25, No. 9, Sept. 1958, pp. 544–560.

[9] Weinig, F. S., "Theory of Two-Dimensional Flow through Cascades," *Princeton Series on High Speed Aerodynamics and Jet Propulsion*, Vol. 10, Princeton Univ. Press, Princeton, N.J., 1964, Sec. B, pp. 24–50.

[10] Horlock, J. H., "Axial Flow Compressors," *Fluid Mechanics and Thermodynamics*, Butterworths, London, 1958, pp. 48–51.

[11] McCune, J. E. and Dharwadkar, S. P., "Lifting Line Theory for Subsonic Axial Compressor Rotors," GTL 110, July 1972, Gas Turbine Lab., MIT, Cambridge, Mass.

OCTOBER 1974 AIAA JOURNAL VOL. 12, NO. 10

Part II—Transonic Compressor

The authors' three-dimensional, inviscid, linearized lifting surface theory of compressible flow past an axial compressor rotor is applied to transonic compressors. From the general solution, quasi-two-dimensional limiting forms are obtained for a supersonic blade section. The latter consists of an equivalent actuator-disk type flow due to the azimuthally averaged wake, plus the local two-dimensional supersonic cascade flow. The actual flow is shown to depart considerably from these quasi-two-dimensional flows, even for uniformly loaded rotors. These departures are due to two major factors: namely, the propagation of acoustic waves, and the occurrence of wake induced resonance. These waves influence the flow at all sections of the blade, thus eliminating the sharp differences that would otherwise exist between subsonic and supersonic blade sections. The resonant modes are treated by inclusion of certain nonlinear effects, and the acoustic pressure field is investigated and related to the rotor geometry and aerodynamics. Camber-line profiles are obtained for transonic rotors under specified loading distributions, and blade forms are shown to be very sensitive to the presence or absence of a wake, for a specified mean loading. For uniformly loaded transonic rotors, the blade camber becomes reversed near the sonic radius.

I. Introduction

In part I of the present theory,[1] the three-dimensional, inviscid, linearized lifting surface solution for compressible flow past an axial compressor blade row has been presented. It was shown that, by averaging the three-dimensional flow in the azimuthal direction, the resulting axisymmetric flow showed features of the well-known axisymmetric through-flow (actuator disk) theory. In particular, when the relative Mach number is everywhere subsonic, the general three-dimensional theory was reducible to a quasi-two-dimensional limiting form which was shown to consist of an actuator disk-type flow, on which was superposed the local two-dimensional cascade flow about the blade section. Departures of the actual flow from these quasi-two-dimensional limiting forms were shown to be primarily due to the presence of individual trailing vortices, that is, the rotor wake. Thus, for a uniformly loaded rotor, these quasi-two-dimensional approximations adequately represented the actual flow at each blade section.

These conclusions have recently been reinforced by Namba.[2] Although Namba's assumptions are the same as in the present work, his solution is based on a pressure dipole representation of the blade surfaces, from which the disturbance pressure and the perturbed field everywhere is then sought.

There has always been some doubt as to the applicability of the assumption of quasi-two-dimensionality to transonic rotors.[3] McCune[4] has studied the problem of transonic flow through a nonlifting axial compressor rotor for small values of the thickness to chord ratio. In the study, the blade thickness distribution was represented by radial source spikes of varying strength in the radial direction, and it was shown that the interference between various sections of the blades was considerable, the flow at each section being nowhere near to being quasi-two-dimensional. The primary reason for this radical departure from quasi-two-dimensionality was the acoustic resonance of certain eigenmodes which, when excited, drastically alter the flow at all sections of the blade row.

In the present paper, we make a similar investigation of the lifting transonic rotor, in which the blades, though having camber, will be assumed to have zero thickness. We stay, as before, within the framework of an inviscid, linearized theory. Within this framework, the complete problem is solved by superposition of the solutions of the thickness and lifting problems. For the lifting problem, we identify two major causes of large departures of the actual flow from quasi-two-dimensionality. The first is, as in the thickness problem, the excitation of propagating acoustic eigenmodes when the relative Mach number at the tip sections becomes supersonic. These modes, which propagate whether or not there is a wake behind the rotor make their presence felt at all radial sections, thus altering the essential pattern of the flow even at the hub sections where the relative Mach number is subsonic.

The second cause of departures from quasi-two-dimensionality is the wake. As in the subsonic case, the presence of trailing helical vortex sheets behind the rotor introduces additional induced velocities at each blade section. In the transonic case, however, the wake plays the additional role that it excites propagating acoustic modes, some of which, under certain conditions can become resonant, that is, have very large amplitudes within the linear theory; and when such resonance is excited, the interference between the different radial sections of the blade becomes greatly intensified. Since transonic operation always